Miner Deposita (2015) 50:339–355
DOI 10.1007/s00126-014-0541-4

ARTICLE

The Lac Des Iles Palladium Deposit, Ontario, Canada. Part II. Halogen variations in apatite

Paul Schisa · Alan Boudreau · Lionnel Djon · Arnaud Tchalikian · John Corkery

Received: 17 January 2014 / Accepted: 7 July 2014 / Published online: 9 August 2014

Abstract Analysis of apatite from the Mine Block Intrusion (MBI) of the Lac des Iles Igneous Complex shows two pronounced trends in the halogens. Apatite from relatively fresh norite and melanorites from the Pd-sulfide zone contain up to 57 mol% chlorapatite endmember with significant hydroxyapatite component. In contrast, in altered rock (amphibolite and greenschist assemblages) the chlorapatite component is typically less than 10 mol% with wide variation in the F- and OH-endmember components. The latter trend is attributed to Cl loss to degassing and alteration, whereas the former is attributed to Cl enrichment in the ore-bearing rocks. It is suggested that the relatively H_2O-rich and intermediate Cl content of the early igneous fluids degassed from the deeper levels of the MBI can explain the high Pd/Pt and Pd/Ir ratios of the deposit. A model is presented in which disseminated Pd-rich sulfides are initially introduced by a high-temperature magmatic fluid that also influenced crystallization to produce the gross modal variations of the igneous host rock. This high-temperature mineralization event was subsequently modified by the influx of late igneous and country fluids at amphibolite to greenschist conditions.

Keywords Apatite · Lac des Iles Pd Deposit · Platinum-group elements

Editorial handling: C. Li and B. Lehmann

P. Schisa · A. Boudreau (✉)
Division of Earth & Ocean Sciences, Duke University, Box 90227, Durham, NC 27708, USA
e-mail: boudreau@duke.edu

L. Djon · A. Tchalikian · J. Corkery
Metals Exploration Division, North American Palladium Ltd., 556 Tenth Ave., Thunder Bay, ON P7B 2R2, Canada

Introduction

The Mine Block Intrusion (MBI) of the Lac des Iles Igneous Complex (LDIC) is a small, crudely concentrically zoned igneous body that hosts a significant Pd deposit containing 15 million (+) tons of proven + probable ore reserves averaging 2.77 ppm Pd, 021 ppm Pt 0.20 ppm Au, 0.08 wt% Ni, and 0.06 wt% Cu (North American Palladium website December 2013 resource estimates). Models for its petrogenesis range from those that are strictly magmatic to those that suggest a role by fluids infiltrating across a range of conditions, from magmatic down to greenschist-grade temperatures. In regards to the latter, a number of studies have noted the extensive alteration of the rocks, the pegmatoidal textures, the presence of magmatic breccias, the unusually high Pd/Pt ratio of 12.3, and the very high Pd/Ir ratios (4,500–65,000) of the ores (e.g., Dunning 1979; Talkington and Watkinson 1984; Brügmann et al. 1989; Lavigne and Michaud 2001; Watkinson et al. 2002; Somarin et al. 2009; Hinchey et al. 2005; Hanley and Gladney 2011; Barnes and Gomwe 2011; Djon and Barnes 2012). This has led these authors to propose models in which late magmatic or metamorphic fluids either were the source of the Pd or led to selective upgrading in the high-grade rocks (e.g., Barnes and Gomwe 2011). More recent underground development has found unaltered mineralized norites, casting doubt on the role of amphibolite-greenschist alteration as the main process of ore deposition and instead likely resulted in the degradation of ore grade (Boudreau et al. 2014).

In a number of earlier studies, the halogen geochemistry of igneous minerals, and apatite in particular, has been investigated in a variety of layered intrusions as a potential indicator of those intrusions that may host high-grade platinum-group element (PGE) deposits and to explore the possibility that Cl-rich fluids may have been important in the ore zone petrogenesis. For example, it has been shown that the apatite in the footwall rocks to the major PGE deposits of the Bushveld

Complex (the UG-2 chromitite and the Merensky Reef) and the Stillwater Complex (the J-M reef) contains anomalously high Cl concentrations (e.g., Boudreau et al. 1986; Boudreau and McCallum 1992; Willmore et al. 2000). While there has been some work on fluid inclusions and the halogen-bearing minerals of the heterolithic units and the pegmatoidal amphibolites (Sutcliffe et al. 1989; Hanley and Gladney 2011) and greenschist rocks (Somarin et al. 2009) of the Mine Block Intrusion, there has been no previous work on the halogen geochemistry of the unaltered assemblages.

Part I of this study was a quantitative study of reaction progress with progressive alteration of fresh norite and melanorite protolith and found that alteration mainly leads to a loss of the PGE and base metal sulfides (Boudreau et al. 2014). It was concluded that mineralization was largely a high-temperature event involving either magmatic precipitation of sulfides or an igneous mineralizing fluid above the stability of amphibole. This work reports the composition of apatite from the Mine Block Intrusion and shows the apatite of the unaltered assemblages to be intermediate between the Cl-rich apatite of the Bushveld and Stillwater complexes and the typically Cl-poor (<10 mol% chlorapatite component) found in most other intrusions. It is suggested that the lack of high Cl and CO_2 concentrations in the MBI fluid strongly limited the transport of the less soluble Ir, Os and Ru (= IPGE) and can explain the high Pd/Ir ratio of the MBI mineralization.

Geology and previous work

General descriptions of the regional geology of the area covered by the LDI suite intrusions can be found in Pye (1968), Sutcliffe et al. (1989), and Stone et al. (2003). The LDIC is located approximately 80 km north of Thunder Bay, Ontario. The complex is part of the Lac des Iles Suite, whose mafic intrusive rocks generally range in age between 2,686 and 2,699 Ma (Stone 2010). These rocks have intruded a variety of metamorphosed granitoid and supracrustal greenstone belt rocks (ca. 2.9 to 2.7 Ga in age) of the Wabigoon Subprovince of the Superior Province. The LDIC lies immediately north of the boundary between the volcano-plutonic Wabigoon and metasedimentary Quetico subprovinces. It is the largest of a series of mafic and ultramafic intrusions that occur along the boundary that collectively define a 30-km-diameter circular collection of intrusions (Lavigne and Michaud 2001) (Fig. 1).

The Lac des Iles Complex has been traditionally subdivided into three distinct bodies: the North Lac Des Iles Intrusion (NLDI), the MBI, and the Camp Lake Intrusion (Brügmann et al. 1989; Lavigne and Michaud 2001). The North Lac des Iles Intrusion is a complex polyphase intrusive body likely consisting of a series of nested to locally cross-cutting intrusions composed predominantly of ultramafic rock (olivine-rich to orthopyroxene-rich). The MBI is located in the central part of the LDIC and is composed of a variety of mafic rock types, while the Camp Lake Intrusion is predominantly composed of a homogenous mafic rock (typically described as a hornblende gabbro, e.g., Brügmann et al. 1989) and is located southwest of Camp Lake. The economic, Pd-dominant PGE deposits are hosted entirely by the MBI, where at the surface, they are associated with lithologically and texturally complex package of rocks typically defined as "gabbroic" (but see below) (Lavigne and Michaud 2001; Hinchey et al. 2005; Barnes and Gomwe 2011). More recent work by North American Platinum Geologist has defined the South Lac Des Iles Intrusion (SLDI) as separate from the rest of the Camp Lake Intrusion. The SLDI is a predominantly mafic intrusion having many similarities to the MBI in terms of rock types and textures but is currently not known to contain significant mineralization. The boundary between the MBI and the SLDI is not well defined.

Within the MBI, the Offset Fault separates the Roby Block to the north and the smaller Offset block to the south; the Roby Block appears to be roughly one third of an originally circular intrusion that has been truncated by the Offset Fault. The Offset Fault itself is one of several northwest-dipping ~45° reverse faults thrusting deeper portions of the complex over shallower. This suggests that all four intrusions were originally part of one single intrusion with the ultramafic North LDI Intrusion originally below the MBI and the SLDI and the Camp Lake Intrusion being the upper, more fractionated parts of the original intrusion. However, rarely observed intrusive contacts between the NLDI and the MBI suggest that the NLDI was younger.

An idealized cross section of the MBI is shown in Fig. 2. As noted, the rocks seen at the surface and extending part way into the open pit is a complex package of lithologically and texturally variable rocks whose relationships can be difficult to unravel owing in part to poor exposure. Beneath this zone, drilling and mine development shows the radial stratigraphy to be considerably simpler. However, even here the pervasive alteration in many of the rocks (ranging from amphibolite to greenschist facies assemblages) and the tendency of previous authors to name the rocks based on inferred original lithology have led to considerable confusion in the literature and a difficulty in correlating some unit. In particular, the alteration to green amphibole has led to the description of many rocks as "gabbro," although rocks that might be defined as true gabbro only occur in the most evolved units that typically occupy the interior/upper portions of the bodies. This is evident when comparing the logged rock names and the Cross, Iddings, Pirsson and Washington (CIPW) normative components shown

Fig. 1 Regional geology showing the igneous intrusions in the eastern Wabigoon Subprovince. *Inset:* Simplified geologic map of the Lac des Iles Igneous Complex. Modified after Brügmann et al. (1989, 1997) and Lavigne and Michaud (2001)

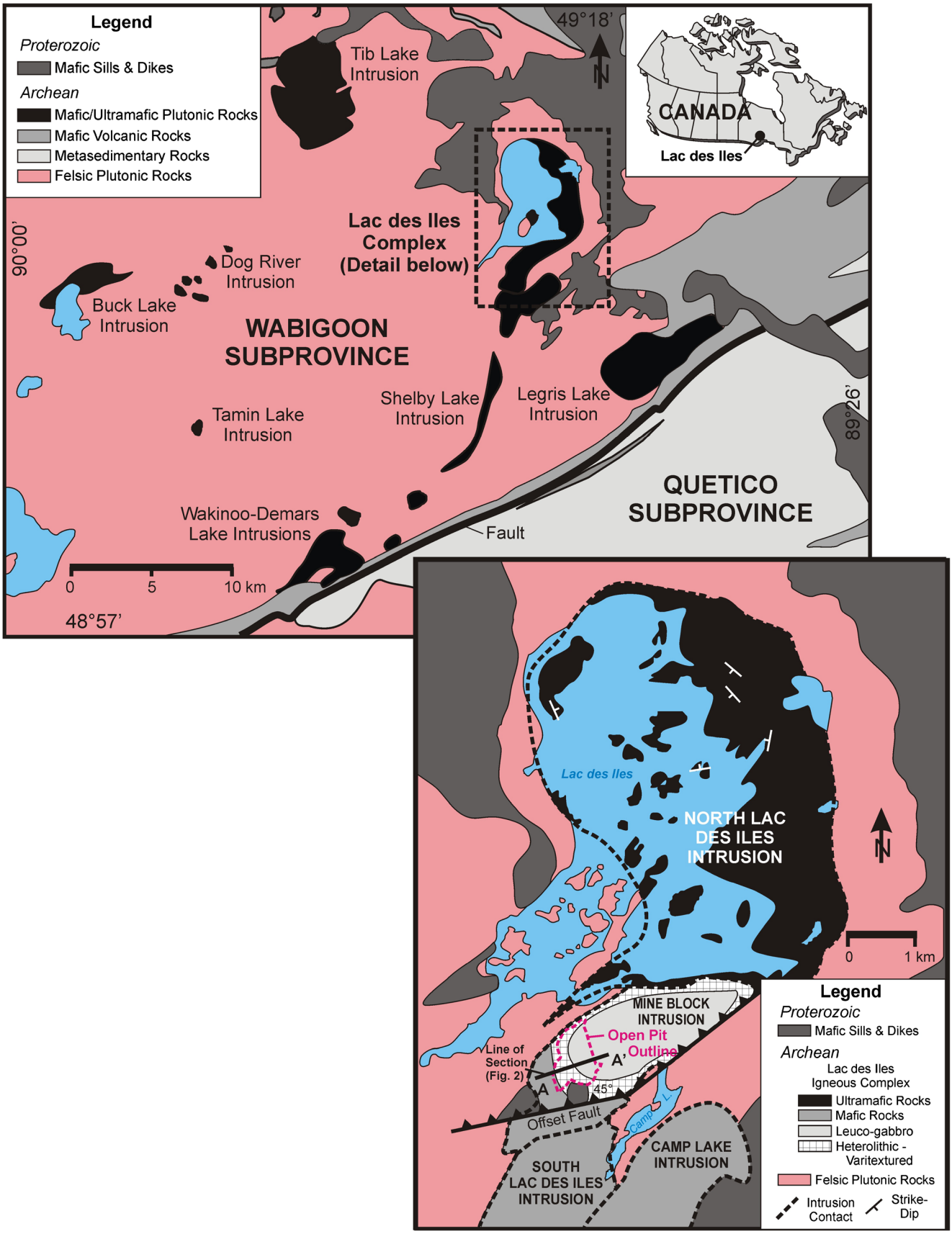
Legend
Proterozoic
Mafic Sills & Dikes
Archean
Mafic/Ultramafic Plutonic Rocks
Mafic Volcanic Rocks
Metasedimentary Rocks
Felsic Plutonic Rocks
49°18'
90°00'
89°26'
48°57'
N
CANADA
Lac des Iles
Tib Lake Intrusion
Lac des Iles Complex (Detail below)
Dog River Intrusion
Buck Lake Intrusion
WABIGOON SUBPROVINCE
Tamin Lake Intrusion
Shelby Lake Intrusion
Legris Lake Intrusion
QUETICO SUBPROVINCE
Wakinoo-Demars Lake Intrusions
Fault
0 5 10 km
Lac des Iles
NORTH LAC DES ILES INTRUSION
0 1 km
MINE BLOCK INTRUSION
Open Pit Outline
Line of Section (Fig. 2)
A
A'
45°
Offset Fault
Camp L.
CAMP LAKE INTRUSION
SOUTH LAC DES ILES INTRUSION
Legend
Proterozoic
Mafic Sills & Dikes
Archean
Lac des Iles Igneous Complex
Ultramafic Rocks
Mafic Rocks
Leuco-gabbro
Heterolithic - Varitextured
Felsic Plutonic Rocks
Intrusion Contact
Strike-Dip

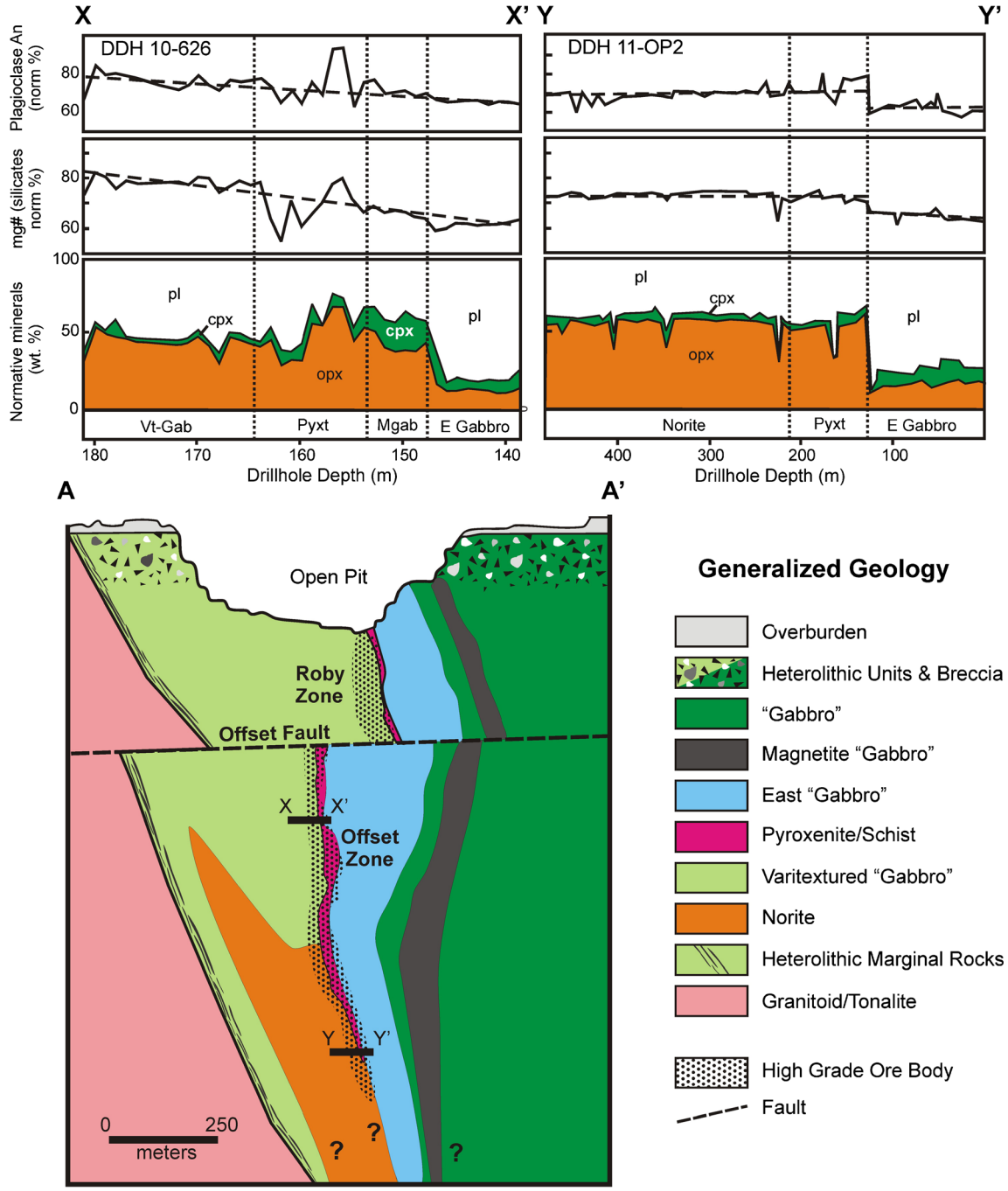

Fig. 2 Example drill core profiles through the mineralized rocks of the Mine Block Intrusions (*top*) and a generalized cross section (*bottom*, simplified after Duran et al. 2012) through part of the Mine Block Intrusion of the Lac des Iles Complex. For the drillhole sections, the *right* is toward the center of the MBI. Lithology noted at the *bottom* is as logged and is compared with the calculated CIPW normative mineralogy, normative An# of plagioclase, and Mg# of pyroxene and illustrates the problem of inferring original lithology of altered rocks. Abbreviations: *Vt-Gab* = varitextured "gabbro"; *Pyxt* = pyroxenite; *Mgab* = mela-"gabbro"; *E Gabbro* = East Gabbro

in Fig. 2. With these caveats, from the margins inward, the rocks at the deeper levels are comprised of the following major units as mapped by North American Palladium geologist.

Marginal zone Although not mapped as a distinct unit, the rocks near the contact with the country rock are composed of a heterolithic variety of rocks that are similar to the features seen in the Marginal Border Group of the Skaergaard Intrusion (e.g., Hoover 1989). These include pegmatoids, variably developed modal layering, possible metasomatic replacement bodies, and the presence of xenoliths of the tonalite country rock.

Varitextured "gabbro" unit Away from the marginal contacts is a distinctive rock that is generally describes as a varitextured

"gabbro" but which is properly termed a plagioclase amphibolite. It is typically a medium-grained (locally coarse-grained to pegmatitic) rock with centimeter-size regions of that are textural coarser than the rest of the rock. Mineralogy is mainly dominated by amphibole replacing orthopyroxene and plagioclase with a variable greenschist overprint. The plagioclase grains are subhedral (range from 2 to 7 mm) and make up between 40 and 60 modal%, whereas primary amphibole grains are generally subhedral to rounded and make up between 30 and 40 modal%. Most grains of plagioclase are slightly–moderately altered to sericite and chlorite along fractures or at the contact with minerals, and some grains of amphibole altered to chlorite or biotite. Locally, secondary magnetite and pyrite occur as fine, disseminated and occasionally larger, single grains. The presence of relic orthopyroxene in the cores of magnesiohornblende/cummingtonite, the similar bulk rock compositions as the norite (see below), and CIPW normative compositions (Fig. 2) imply a norite protolith. This unit can be variably mineralized.

Norite unit At deeper levels and where rocks have not experienced the extensive amphibolitization, the rocks are a medium grain norite of more uniform texture than the varitextured "gabbro." As with the vartitextured "gabbro," this unit may be variably mineralized. Orthopyroxene average 65 vol% but can be as high as 90 % in the melanorites. Clinopyroxene is less abundant and averages ~15 % by volume and is present either as subhedral grains in association with orthopyroxene or either as lamellae (or inclusion) within orthopyroxene grains. Plagioclase varies from 10 % (in melanorite) to 65 % (in leuconorite).

An intermediate rock between norite and the varitextured gabbro is locally logged as a varitextured gabbronorite. These have textures and mineralogy similar to varitextured gabbro. However, most amphibole grains are more clearly secondary and are more likely to only partially replace pyroxene.

"Pyroxenite" unit This is a strongly altered and locally strongly sheared unit that is properly termed a chlorite + tremolite ± talc schist. CIPW normative composition implies that the protolith was a melanorite to norite, the latter having perhaps more extensive alteration and shearing than is seen in the varitextured "gabbro" and norite units. The higher Pd grades tend to be associated with this rock as well as in the immediately adjacent varitextured "gabbro" and norite units.

East "gabbro" unit Again, the pyroxenes in this unit are typically altered to green hornblende leading to its description as a gabbro. The mineralogy is plagioclases (40 %), amphiboles (30 to 35 %), and pyroxenes (10 to 15 %). CIPW normative mineralogy suggests the protolith was a leuco (gabbro) norite, and relicts show that there are more orthopyroxene than clinopyroxene (Djon and Barnes 2012). It is the litho-mechanical contrast between this leucocratic unit and the pyroxenite unit that causes the pyroxenite to preferentially faulted and more strongly altered. This unit is the most extensive/continuous and also generally marks the inward limit of mineralization.

"Gabbro" and magnetite "gabbro" units Further in toward the core of the intrusion are rocks of uncertain radial extent that have been described as medium-grained gabbro and magnetite gabbro.

The main zone of mineralization in the MBI as expressed at the surface, the Roby Zone, includes the High-Grade Zone (defined as >4 ppm Pd) (Gomwe 2008; Barnes and Gomwe 2011; Djon and Barnes 2012) and occurs as an arc of mineralized rocks that occur on the western side of the MBI. Barnes and Gomwe (2011) describe the Roby Zone (and the nearby Twilight Zone) as consisting of apparently magmatic heterolithic breccias of gabbronorite or metagabbronorite, which contain pegmatoidal and varitextured patches along with extensive amphibolitization. The High-Grade Zone is a 15- to 30-m-wide Pd-rich zone (mean concentration of 7.89 ppm Pd; Watkinson et al. 2002) located between the Roby zone breccia and the East Gabbro and is the primary ore target (Lavigne and Michaud 2001).

Within these broad averages, the grades can be highly variable, ranging from 0 to greater than 120 ppm Pd over a 1-m interval. As Pd grade increases, the Pt plateaus at about 3 ppm. This results in systematic variation in the Pd/Pt ratio which can be close to 1:1 at the very lowest grades (sub-1 ppm) and increases to 40 to 50:1 at the highest Pd grades. With these caveats, the major rock types show the following typical grades and ranges. Varitextured "gabbro" ranges from 0 to 65 ppm Pd with the average grades between 1 and 4 ppm Pd. Pyroxenite varies from 0 to >120 ppm Pd with average grades between 8 and 12 ppm Pd. Fresh norite ranges between 0 and 15 ppm Pd with averages between 3 and 6 ppm Pd. East Gabbro mineralization is very rare and occurs mostly along faults where it may reach 5 ppm.

Beginning about 2010, mining commenced underground on the Offset Zone, a fault offset of the overlying Roby Zone. Extensive drilling and ongoing mine development shows that the breccias and the complex lithological units that characterize much of the upper parts of the Roby Zone are much less evident at these deeper levels. This suggests that the heterolithic units seen near the surface and extending only partly down into the open pit may have played a less important role in the formation of the ore deposit than previously thought. Specifically, the rootless character to the heterolithic bodies cast doubt on the interpretation that they formed by influx of exogenetic magmas (e.g., Hinchey et al. 2005; Hinchey and Hattori 2005) and are perhaps more akin to the contrasting mafic/felsic replacement bodies seen in the Skaergaard, for example (McBirney and Sonnenthal 1990).

In addition, drilling and mine development at the deeper levels have found more of the mineralized medium-grained norite in which the amphibolite-greenschist overprint is much reduced.

Methods

Because of the trace nature of the hydrous minerals in the fresher samples, a combined SEM–microprobe study was used to locate and characterize these minerals. Microprobe analyses were performed on polished thin sections using the Cameca Camebax electron microprobe at Duke University, Durham, NC, USA. Typical analytical conditions were 15 KeV acceleration voltage, 15 nA beam current, and a focused to 10 μm beam diameter. Peak and background counting times for Cl ranged from 20–30 and 10–15 s, respectively. Other elements were counted on the peak for 30 s and background for 15 s. To minimize volatilization/element migration during beam bombardment, F and Cl were counted first. Standards included a synthetic apatite (supplied by Adam Simon of UNLV) and natural chlorapatite (RM-1, Morton and Catanzaro 1974) and fluorapatite (from Wilberforce, Ontario) for Ca, P, and the halogens, as well as a variety of silicate mineral standards. Allanite (102522, #42; Frondel 1964) was used for La and Nd for which the analyte lines are relatively free from overlap (Roeder 1985); other rare earth elements (REE) were not analyzed owing to the low concentration of the REE in general. F and Cl in the apatite standards were checked against fluorite, topaz, and halite. Fluorine was analyzed using a synthetic Si-W-layered diffracting crystal. OH^- and H_2O were calculated by difference based on hydroxyl site occupancy. Previous work with these analytical conditions (Willmore et al. 2000) has shown no significant apatite orientation effects on the analyses as has been observed by Stormer et al. (1993).

Bulk rock analysis was done by lithium metaborate/tetraborate fusion ICP/MS and routine PGE analysis by NiS fire-assay ICP-MS, both by Actlabs, Thunder Bay, Ontario. North American Palladium verifies the Actlabs' results using a variety of standards from CDN Resource Laboratories, Ltd. These include using a CDN blank (CDN-BLK-XX), and both a high and low PGM standards (CDN-PGMS-XX). A very clean white marble is used to control the cleanliness of the Actlabs' sample preparation.

Results

Petrology of late-crystallizing minerals

In the unaltered rocks, the halogen-bearing minerals, and apatite in particular, are present in only minor modal amounts. Apatite is the principal mineral of interest as it is a commonly occurring halogen-bearing mineral and, more importantly, halogen substitution in apatite is likely ideal at high temperatures (>500 °C) (Tacker and Stormer 1989; but also see Hovis and Harlov 2010). The apatite grains analyzed in this study are interstitial to plagioclase and orthopyroxene but are only locally associated with other minor late-crystallized minerals such as quartz, biotite, and magnetite. In agreement with the low whole-rock concentrations of P_2O_5 (Table 1), the modal abundance of apatite is generally low, with only a few small grains seen in any thin section. The low modal abundance, the interstitial nature, and the lack of apatite as inclusions in the cores of the plagioclase and orthopyroxene all point to the late crystallization of apatite from small amounts of evolved residual liquid.

Although many of the norite samples appear fresh in hand sample, all samples show some minor alteration to amphibolite/greenschist assemblages. This alteration is usually localized along grain boundaries, around sulfides, or along narrow veins that are typically only a few tens of microns wide. In general, apatite grains that have not been affected by this later alteration have higher Cl concentrations than do those grains where there is extensive alteration in the surrounding silicates.

In most instances, apatite has a stubby habit and is typically no more than a few tens of microns in maximum dimension. As observed in other intrusions, they tend to be clustered within a thin section and not randomly distributed and have been explained by late interstitial melts becoming localized to channels during compaction (e.g., Meurer and Meurer 2006). In one instance, an apatite grain is observed to be cut by a small talc-magnetite vein and has markedly higher Cl concentrations next to the vein on one side but not on the other (Fig. 3). This sample is also the only instance where biotite was found in contact with apatite. The paucity of apatite–biotite pairs in contact meant that apatite–biotite geothermometer measurements could not be made.

Apatite composition

Representative apatite analyses are presented in Table 2, and the F-OH-Cl variations are shown in Fig. 4. A file with all apatite analysis is available as online supplementary material. Overall, the apatite compositions define two distinct trends, one defined by variable Cl concentrations that range from distinctly Cl-enriched (X^{Cl}=0.57 maximum) to about 10–20 mol% Cl endmember that runs roughly parallel to the Cl-OH sideline, and the other is a Cl-poor trend (<10 mol% Cl) that is defined mainly by F-OH variation. The first trend is characteristic of the "fresh" norites and melanorites and some of the varitextured rocks that still have some unaltered pyroxene, whereas the Cl-poor trend is typical of those rocks in

Table 1 Representative bulk rock analysis

Sample	10-628-164	00-214-473	11-700-021	10-814-255	11-609 146	11-705-089	05-001-204	10-615 -167	10-766-143	01-020 253	05-005-216	10-507-1108
Lithology[a]	vt-gabbro	Norite	Melanorite	Norite	Gabbronorite	Norite	Gabbro	vt-gabbro	vt-gabbro	Gabbro	Gabbro	mt-gabbro
Alteration[b]	Amph.	Altered	Fresh	Fresh	Fresh	Fresh	Amph.	Amph.	Amph.	Amph.	Amph.	Altered
SiO_2	48.34	51.11	51.48	51.48	49.52	49.57	50.09	48.66	48.30	49.76	48.98	38.75
TiO_2	0.10	0.13	0.17	0.15	0.09	0.19	0.16	0.09	0.09	0.19	0.15	1.29
Al_2O_3	21.42	17.07	9.94	12.93	17.15	11.72	21.84	19.56	21.30	12.62	22.86	19.41
FeO[c]	4.49	6.82	10.81	9.72	6.43	14.06	6.08	5.98	5.14	10.59	5.84	20.25
MnO	0.09	0.13	0.19	0.18	0.12	0.20	0.01	0.11	0.10	0.17	0.08	0.10
MgO	7.84	9.97	17.77	14.47	10.59	14.01	5.87	10.15	6.97	13.48	5.83	5.69
CaO	11.33	9.78	6.37	8.05	10.10	7.42	11.81	10.75	11.29	7.83	11.33	8.50
Na_2O	1.89	1.99	0.86	1.37	1.69	1.13	2.50	1.34	1.94	1.01	2.15	1.60
K2O	0.54	0.32	0.22	0.11	0.19	0.09	0.22	0.35	0.27	0.26	0.18	0.21
P_2O_5	0.01	0.01	0.01	0.01	0.01	0.01	0.01	0.01	0.01	0.01	0.01	0.01
Cr_2O_3	0.03	0.03	0.07	0.06	0.03	0.04	0.01	0.04	0.03	0.04	0.06	0.21
S	0.06	0.27	0.03	0.10	0.25	1.28	0.06	0.31	0.35	0.03	0.02	0.01
LOI	3.21	2.90	1.41	0.78	2.98	0.76	1.31	3.15	2.91	3.82	1.89	1.64
Total	99.4	100.5	99.3	99.4	99.2	100.5	100.1	100.5	98.7	99.8	99.4	97.7
Bulk Mg#	75.7	72.3	74.6	72.6	74.6	64.0	63.2	75.2	70.7	69.4	64.0	45.3
CIPW norm												
an+ab+or	67.6	55.4	31.2	41.1	54.1	36.7	70.2	59.7	66.6	39.2	71.5	56.9
hy	15.1	31.1	54.9	44.6	29.5	46.7	13.9	26.8	20.2	46.6	19.4	11.5
di	6.3	9.5	7.2	9.0	9.2	8.2	8.9	5.6	5.9	7.8	3.2	0.0
ol	6.8	0.4	4.1	3.4	2.4	3.5	5.2	4.0	1.7	1.8	3.0	1
py	0.16	0.74	0.08	0.27	0.69	3.51	0.16	0.85	0.96	0.08	0.06	0.03
ilm	0.2	0.2	0.3	0.3	0.2	0.4	0.3	0.2	0.2	0.4	0.3	2.5
An#	74.0	67.3	74.5	70.1	71.8	72.4	68.0	79.4	73.6	76.3	73.0	74.6
Mg# hy	75.7	74.0	74.6	73.0	76.2	69.0	63.9	77.3	73.9	69.5	64.4	57.3 (mt=11.6)[d]
Trace elements (ppm)[e]												
Sc	18	29	39	37	25	38	26	23	18	36	18	16
V	75	111	166	126	83	166	126	86	74	192	147	1,856
Cr	200	220	520	380	200	300	70	250	210	290	420	1,430
Co	40	65	87	82	68	135	38	56	60	76	40	101
Ni	645	744	470	380	860	2,190	129	1,310	1,190	385	175	460
Cu	142	913	40	220	770	2,810	81	1,190	1,080	152	64	22
Zn	26	36	80	80	40	100	30	28	26	50	27	58
Pd	1.89	2.55	0.1	0.0017	0.36	5.22	0.0168	5.82	4.47	0.137	0.0552	0.0986
Pt	0.169	0.199	0.0321	0.0007	0.135	0.693	0.0081	0.375	0.375	0.0183	0.0079	0.0076
Ag	0.15	0.6	0.25	0.25	0.25	.7	0.15	0.15	0.15	0.15	0.15	0.15
Au	0.025	0.241	0.005	0.002	0.225	0.605	0.004	0.343	0.138	0.009	0.003	0.002

Table 1 (continued)

Sample	10-628-164	00-214-473	11-700-021	10-814-255	11-609 146	11-705-089	05-001-204	10-615 -167	10-766-143	01-020 253	05-005-216	10-507-1108
Lithology[a]	vt-gabbro	Norite	Melanorite	Norite	Gabbronorite	Norite	Gabbro	vt-gabbro	vt-gabbro	Gabbro	Gabbro	mt-gabbro
Alteration[b]	Amph.	Altered	Fresh	Fresh	Fresh	Fresh	Amph.	Amph.	Amph.	Amph.	Amph.	Altered
Pb	2.5	2.5	2.5	2.5	2.5	2.5	2.5	2.5	2.5	2.5	2.5	6
Rb	16	9	6	1	6	1	7	14	9	9	5	5
Sr	226	205	109	139	185	143	259	174	241	89	252	212
Y	2	2	1	3	2	2	3	2	1	2	1	1
Zr	7	8	4	7	5	2	8	5	4	8	4	6
Nb	2	0.5	0.5	0.5	0.5	.5	.5	0.5	0.5	0.5	0.5	0.5
Cs	3.3	2.3	2.1	0.25	1.7	1.1	3	3.9	2.6	2	2	3.2
Ba	113	73	40	36	42	28	61	44	50	41	42	47
La	2.1	1.5	1.1	5.3	4.3	0.8	1.1	0.7	1.4	1.2	1	0.6
Ce	3.7	2.9	2.1	3.6	2.8	1.5	2.3	1.5	2.5	2.6	1.9	1.2
Pr	0.42	0.34	0.25	0.38	0.27	0.19	0.28	0.18	0.27	0.31	0.2	0.13
Nd	1.5	1.4	1.1	1.6	1.0	0.8	1.3	0.8	1.0	1.3	0.8	0.5
Sm	0.3	0.3	0.2	0.4	0.2	0.2	0.3	0.2	0.2	0.3	0.2	0.05
Eu	0.14	0.2	0.13	0.18	0.12	0.15	0.22	0.12	0.15	0.14	0.12	0.1
Gd	0.3	0.3	0.3	0.5	0.3	.3	0.3	0.2	0.2	0.3	0.2	0.1
Tb	0.05	0.05	0.05	0.05	0.05	.05	0.05	0.05	0.05	0.05	0.05	0.05
Dy	0.3	0.4	0.4	0.6	0.3	.4	0.4	0.3	0.2	0.4	0.2	0.1
Ho	0.05	0.05	0.05	0.1	0.05	.05	0.05	0.05	0.05	0.05	0.05	0.05
Er	0.2	0.3	0.3	0.5	0.2	.3	0.2	0.2	0.2	0.3	0.1	0.05
Tm	0.025	0.025	0.025	0.07	0.025	.05	0.025	0.025	0.025	0.025	0.025	0.025
Yb	0.2	0.3	0.4	0.5	0.3	.4	0.3	0.2	0.2	0.3	0.2	0.05
Lu	0.02	0.05	0.06	0.09	0.05	0.06	0.04	0.04	0.02	0.05	0.02	0.02
Hf	0.1	0.2	0.1	0.2	0.1	.1	0.1	0.1	0.1	0.1	0.1	0.1
Ta	0.05	0.05	0.05	0.05	0.05	0.05	0.05	0.05	0.05	0.05	0.05	0.05
Th	0.4	0.2	0.05	0.1	0.1	.05	0.2	0.05	0.2	0.2	0.05	0.05
Bi	1	0.2	0.2	0.2	0.2	0.2	0.2	0.6	0.2	0.2	0.2	0.2
Ga	12	11	9	10	10	10	16	11	13	10	17	26
Sb	0.25	0.25	0.25	0.25	0.25	0.6	0.25	0.25	0.25	0.25	0.25	0.25

vt-gabbro varitextured gabbo, *mt-gabbro* magnetite gabbro, *amph.* rock extensively altered to plagioclase amphibolite, *altered* partial greenschist alteration overprint, especially of mafic minerals, *fresh* generally unaltered but may show small veins or local patches of amphibolite/greenschist alteration

[a] Lithology as logged

[b] Alteration and explanation

[c] Total iron calculated as FeO

[d] Sample 10-507-1108: total iron divided between FeO (12.25 wt%) and Fe_2O_3 (8.0 wt%) to make 11.6 wt% mt in the CIPW norm to correct for the 10–15 % modal magnetite in this sample

[e] Analyzed trace elements that fall at and below detection limits for all samples include As (≤2.5 ppm), Be (≤0.5 ppm), Sn (≤0.5 ppm), Ta (≤0.05 ppm) Tl (≤0.05 ppm), U (≤0.05 ppm), and W (≤0.5 ppm)

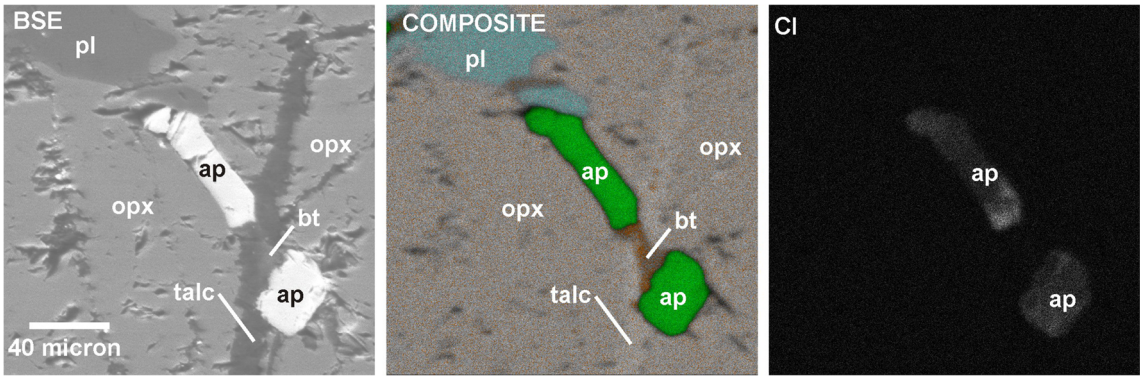

Fig. 3 Sample 11-051-793 (norite). Apatite cut by a small talc-biotite vein. Abbreviations: *pl* = plagioclase; *px* = low Ca pyroxene; *bt* = biotite; *ap* = apatite. Note higher Cl in apatite next to vein

which the alteration is more pervasive and amphibolitization of the pyroxene is more complete. These latter samples substantially overlap the apatite field from amphibolite pegmatoids defined by Hanley and Gladney (2011) and two apatite analyses from an altered sulfide-bearing "gabbronorite" reported by Sutcliffe et al. (1989).

For those samples for which whole-rock analyses are available, a plot of molar Cl/(Cl + F) of apatite against the bulk Mg# in apatite shows that the fresher mineralized samples typically have higher Cl/(Cl + F) molar ratios than do the altered and/or barren rocks at similar bulk rock Mg# (Fig. 5). There is otherwise no clear trend as a function of Mg#, although samples with low (more evolved) Mg# are limited.

Except for the grain cut by a microvein noted above, no measurable compositional zoning was noted in any elements in individual apatite grains, but different grains from the same thin section can vary considerably in composition. This behavior is typical of the compositions of interstitial apatite in other mafic-ultramafic layered intrusions such as the Stillwater and Bushveld complexes (e.g., Meurer and Boudreau 1996; Willmore et al. 2000). This variation has been attributed to a combination of in situ fractionation as individual apatite grains become isolated from the crystallizing interstitial liquid at different times and removal of any primary zoning by diffusion on cooling. In contrast, "cumulus" apatite found in the topmost sections of intrusions such as the Bushveld tends to be more uniform in composition, which Willmore et al. (2000) suggested was the result of these grains having grown from a larger mass of more uniform liquid composition. These wide compositional variations in interstitial apatite make it difficult to determine small scale litho-stratigraphic trends in halogen content to the degree one might discern with, for example, plagioclase compositions. Because of this, individual grain compositions tend to be less important than compositional trends seen in a given sample.

Also shown in Fig. 4 are the ranges of halogen concentrations observed in the Bushveld and Stillwater complexes, the Great Dyke of Zimbabwe, the Munni Munni of Australia, the Kläppsjö Intrusion of Sweden, and the Skaergaard Intrusion. The two former intrusions are unusual in that the thick sections beneath the major PGE reefs, the Merensky Reef in the case of the Bushveld Complex and J-M Reef in the case of the Stillwater Complex, are characterized by unusually Cl-rich apatite. In many samples, the apatite may contain no measurable F (e.g., Boudreau and McCallum 1992). A few of the Mine Block samples do have Cl-rich compositions similar to the Bushveld and Stillwater intrusions. However, the Cl-enriched grains tend to have lower Cl overall and are more OH-rich than for these two intrusions.

The MBI apatite trends are most similar to those of the Kläppsjö Intrusion, Sweden, as reported by Meurer et al. (2004). They noted that apatite compositions in the Kläppsjö define two groups similar to those of the MBI: One contains a mixture of chlorapatite and hydroxyapatite, with <0.3 mol fraction fluorapatite in apatite. These Cl-enriched apatites are found exclusively in ultramafic rocks where it is associated with PGE-sulfide enrichment. In contrast, apatite-group minerals from barren gabbroic rocks are OH-F-dominant, with X^{Cl}<0.25 (Fig. 4).

Discussion

As has been discussed previously (Boudreau and McCallum 1989), variation in halogen abundances in interstitial apatite in intrusions that are not fractionating hydrous minerals is best explained by one of two mechanisms. The first is degassing during crystallization, which tends to drive the apatite toward fluorapatite by vapor loss owing to the different portioning behaviors of F (vapor-incompatible) and Cl (vapor-compatible) in silicate melts (e.g., Mathez and Webster 2005). The second is Cl addition, which can occur as Cl degassed from vapor-saturated regions in the crystal pile migrates to hotter, vapor-undersaturated interstitial liquids where it redissolves. In this regard, the apatite compositional trend along the F-OH sideline is interpreted as largely a function of degassing and loss of Cl.

Table 2 Electron microprobe analysis of apatite from the Mine Block Intrusion of the Lac des Iles Complex

Sample	11-700-021	11-101-653				11-051-793						10-814-255A
	Melanonorite	Sulfide melanonorite				Sulfide noriite						Norite
	Fresh	Fresh				Fresh						Fresh
CaO	54.07	54.93	54.97	55.07	55.19	54.58	53.91	53.47	55.86	55.20	54.77	55.98
P_2O_5	41.09	41.30	40.35	42.88	41.18	41.97	41.08	40.25	41.53	41.41	41.53	40.21
Nd_2O_3	0.05	0.07	0.01	0.01	0.06	0.05	0.04	0.05	0.00	0.01	0.01	0.00
Ce_2O_3	0.10	0.05	0.09	0.09	0.03	0.16	0.06	0.03	0.00	0.07	0.11	0.00
Cl	2.98	1.32	1.41	1.43	2.42	1.51	3.90	3.90	1.36	1.39	1.71	0.27
F	0.24	1.19	1.07	0.58	0.40	0.94	0.35	0.35	1.07	0.89	1.31	1.18
H_2O	0.87	0.87	0.90	1.13	0.97	0.92	0.58	0.56	0.94	1.00	0.70	1.17
Total	99.40	99.72	98.81	101.19	100.25	100.13	99.92	98.61	100.77	99.98	100.15	98.81
O=F, Cl	0.77	0.80	0.77	0.57	0.72	0.74	1.03	1.03	0.76	0.69	0.94	0.56
Total	98.63	98.92	98.04	100.62	99.53	99.39	98.89	97.59	100.01	99.29	99.21	98.25
Mole fractions												
X_{Cl}	0.44	0.19	0.21	0.20	0.35	0.22	0.57	0.58	0.19	0.20	0.25	0.04
X_F	0.06	0.32	0.29	0.15	0.11	0.25	0.09	0.10	0.29	0.24	0.35	0.32
X_{OH}	0.50	0.49	0.52	0.63	0.55	0.52	0.33	0.33	0.53	0.57	0.40	0.67
Cl/OH	0.87	0.39	0.40	0.32	0.64	0.42	1.72	1.76	0.36	0.35	0.62	0.06
Cl/F	6.80	0.60	0.70	1.31	3.23	0.86	6.05	6.02	0.68	0.83	0.70	0.12
Bulk Mg#	0.75	NA	NA	NA	NA	NA	NA	NA	NA	NA	NA	0.73
Sample	00-214-473 Norite Partly altered											
CaO	57.29	56.55	54.49	56.05	56.26	56.67	56.40	55.76	56.90	56.48	55.73	56.32
P_2O_5	40.83	41.44	40.76	41.65	41.04	41.52	42.14	41.18	41.79	40.35	39.78	38.93
Nd_2O_3	0.13	0.02	0.01	0.01	0.00	0.00	0.03	0.02	0.01	0.00	0.00	0.00
Ce_2O_3	0.10	0.08	0.11	0.05	0.09	0.01	0.04	0.08	0.04	0.08	0.04	0.00
Cl	1.35	1.08	3.52	0.79	3.10	0.66	1.20	1.17	0.87	1.12	1.61	1.06
F	0.94	0.76	0.26	1.10	0.21	0.43	0.35	0.33	0.68	1.38	0.97	1.02
H_2O	1.05	1.18	0.73	1.08	0.92	1.45	1.34	1.34	1.28	0.88	0.92	1.06
Total	101.69	101.11	99.88	100.74	101.61	100.75	101.49	99.87	101.58	100.28	99.05	98.39
O=F, Cl	0.70	0.56	0.90	0.64	0.79	0.33	0.42	0.40	0.48	0.83	0.77	0.67
Total	100.99	100.54	98.97	100.09	100.82	100.42	101.07	99.46	101.09	99.45	98.28	97.72
Mole fractions												
X_{Cl}	0.19	0.15	0.51	0.11	0.45	0.09	0.17	0.17	0.12	0.16	0.24	0.16
X_F	0.25	0.20	0.07	0.29	0.06	0.11	0.09	0.09	0.18	0.37	0.27	0.28
X_{OH}	0.59	0.66	0.42	0.61	0.52	0.81	0.75	0.76	0.72	0.50	0.53	0.62
Cl/OH	0.33	0.23	1.22	0.19	0.85	0.12	0.23	0.22	0.17	0.33	0.44	0.25
Cl/F	0.77	0.76	7.20	0.38	8.07	0.82	1.86	1.92	0.68	0.44	0.89	0.56
Bulk Mg#	0.72	0.72	0.72	0.72	0.72	0.72	0.72	0.72	0.72	0.72	0.72	0.72
Sample	10-628-164 Varitextured “gabbro” (plagioclase amphibolite) Altered											
CaO		56.29		57.07		55.48		55.71		56.16		55.52
P_2O_5		39.98		38.99		40.27		39.94		39.67		40.59

Table 2 (continued)

Sample	11-700-021	11-101-653		11-051-793			10-814-255A
	Melanonorite	Sulfide melanonorite		Sulfide noriite			Norite
	Fresh	Fresh		Fresh			Fresh
Nd_2O_3		0.03	0.02	0.00	0.02	0.00	0.03
Ce_2O_3		0.02	0.03	0.00	0.00	0.01	0.06
Cl		0.34	0.23	0.46	0.30	0.53	0.57
F		2.20	2.40	1.61	2.03	1.83	1.57
H_2O		0.68	0.64	0.90	0.75	0.80	0.89
Total		99.54	99.38	98.73	98.74	99.00	99.24
O=F, Cl		1.01	1.06	0.78	0.92	0.89	0.79
Total		98.54	98.32	97.95	97.82	98.11	98.45
Mole fractions							
X_{Cl}		0.05	0.03	0.07	0.04	0.08	0.08
X_F		0.60	0.66	0.44	0.56	0.50	0.43
X_{OH}		0.39	0.37	0.52	0.43	0.46	0.51
Cl/OH		0.13	0.09	0.13	0.10	0.17	0.16
Cl/F		0.08	0.05	0.15	0.08	0.16	0.20
Bulk Mg#		0.76	0.76	0.76	0.76	0.76	0.76

In contrast, the trend towards higher Cl observed in the fresher mineralized rocks is interpreted as an example of Cl addition. This is supported by two lines of inference. First, although there are no known sill/dike or chilled margin samples that may be considered to be parental magmas to the MBI, other examples of apatite from sill/dike suites thought to be parental magmas to other intrusions do not have unusually high Cl/(Cl + F) molar ratios. For example, in the Stillwater Complex, the maximum Cl/(Cl + F) ratio of Basal Series sills/dikes contain at most only about half the Cl as seen in the apatite below the J-M Reef (Boudreau and McCallum 1989). Second, as noted by Mathez and Webster (2005), mafic magmas have a limited carrying capacity for Cl; when this saturation limit is reached, Cl must be accommodated by separation of a saline fluid, apatite, or other Cl-bearing phases during solidification. Separation and migration of a saline fluid are an efficient mechanism to enrich interstitial silicate liquids mainly in the Cl component while leaving F concentrations much less affected.

In the case of the Mine Block Intrusion, the locally extensive alteration overprint is also important. Either of these two high-temperature trends, but especially the Cl-enriched apatite, can be modified during hydration/alteration during the formation of amphibolite and greenschist assemblages, pulling apatite compositions toward hydroxyapatite compositions as described by Boudreau and McCallum (1990). They also note that alteration can also lead to the REE, originally hosted by igneous apatite, to be incorporated into monazite during the alteration of chlorapatite to hydroxyapatite, an association reported for the MBI as well (Sutcliffe et al. 1989). The markedly lower Cl/(Cl + F) ratio of apatite in rocks affected by extensive amphibolitization but otherwise having similar bulk rock Mg# as fresh norite (Fig. 5) is interpreted to be the result of Cl loss accompanying alteration.

These three mechanisms for altering the halogen concentrations (degassing, Cl addition, and alteration) are shown schematically in the inset of Fig. 4.

The high Cl in apatite seen in the ore-bearing samples of the MBI is becoming an increasingly common observation in other intrusions with high PGE tenor sulfides (Fig. 6) and is consistent with experimental work demonstrating that Cl can be important for the transport of the PGE. Hsu et al. (1991) demonstrated significant Pd solubility in Cl-bearing aqueous systems, and Fleet and Wu (1992) have shown that the PGEs, particularly Pt and Pd, are appreciably volatile in dry systems in the presence of both Cl and S at 1,000 °C. More recently, the experimentally determined (volatile fluid)/(silicate liquid) partition coefficients for Pt have been found to range across more than four orders of magnitude ($<10^1$ to $\sim10^4$; Hanley et al. 2005; Simon and Pettke 2009; Blaine 2010; Blaine et al. 2005), with values of 10^3 to 10^4 favored by more Cl-rich fluids and by more mafic over more felsic silicate liquid compositions. Blain (2010) also reports a lower but still significant partition coefficient of 1,100 for Ir partitioning into Cl- and CO_2-rich fluids.

Although the nature of metal chloride complexing in high-temperature fluids is still uncertain, these studies suggest that chloride-carbonate fluids are more effective for moving both the PPGE (Rh, Pt, Pd) and to a lesser extent the IPGE (Ir, Ir, Ru) than can more dilute, H_2O-dominant fluids with only

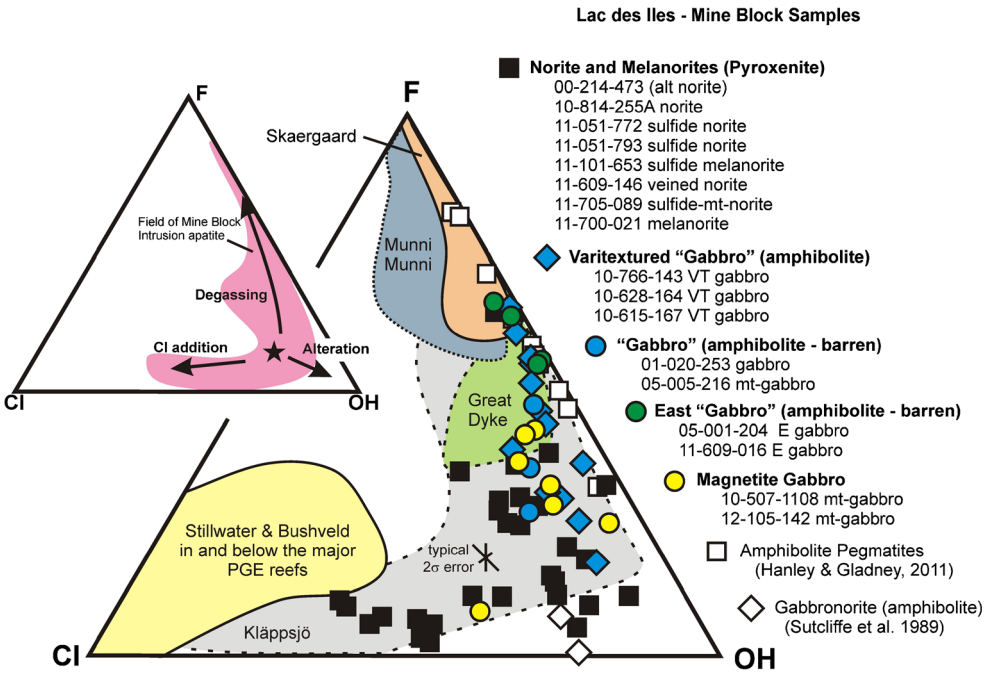

Fig. 4 F-OH-Cl compositional variations in apatite from the Mine Block Intrusion. *Inset:* Halogen compositional trends in apatite as a function of degassing, Cl addition, and hydration due to alteration, as discussed in text. The *star* represents presumed apatite in equilibrium with primitive (undegassed) magma

moderate Cl enrichments. The intermediate chlorapatite component of the MBI apatite (lower than the chlorapatite-rich Stillwater and Bushveld assemblages but higher than the Skaergaard and a number of other intrusions, Fig. 4) and the relatively hydroxyapatite-rich nature of the MBI apatite are consistent with the existence of a Cl-bearing but relatively H_2O-rich (CO_2-poor) fluid and may explain the high Pd/Pt and Pd/Ir ratios of the MBI mineralization. In other words, it is suggested that high concentrations of both Cl and CO_2 are required to move the IPGE and that the intermediate concentrations of these two components in the MBI fluid strongly limited the transport of the less soluble IPGE. This effect could be further enhanced by whatever Pd/Ir variation may have been the result of parent magma variation or PGE fractionation prior to emplacement in the MBI.

Experimental data also confirms the Cl-rich nature of fluids in equilibrium with apatite. For example, as summarized by Webster et al. (2009), the Cl concentration in the fluid is a linear function of X^{Cl} in apatite. Assuming the interstitial liquid at apatite saturation is broadly rhyodacitic in composition, then the fluid in equilibrium with apatite with $X^{Cl}=0.2$ will contain about 20 wt% Cl at ~900 °C. They also note that the co-existing silicate liquids in equilibrium with apatite compositions with mole fraction Cl ranging from 0.2 to 0.5 will contain from 1 to 4 wt% Cl, the higher values more typical of basaltic liquids and the lower for more rhyolitic liquids. For 2 wt% Cl in the melt, Blain et al. (2011) found the high vapor/silicate liquid partition coefficients of 10^3–10^4 for Pt noted above.

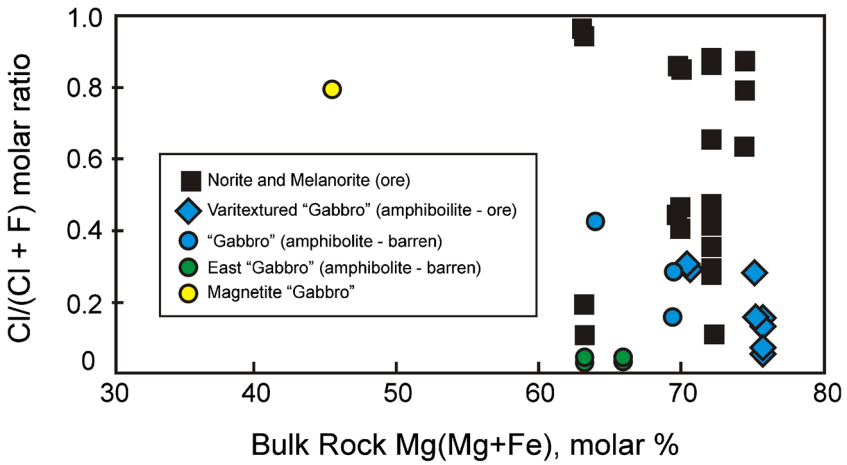

Fig. 5 Plot of Cl/(Cl + F) molar ratio of apatite against the whole-rock Mg#

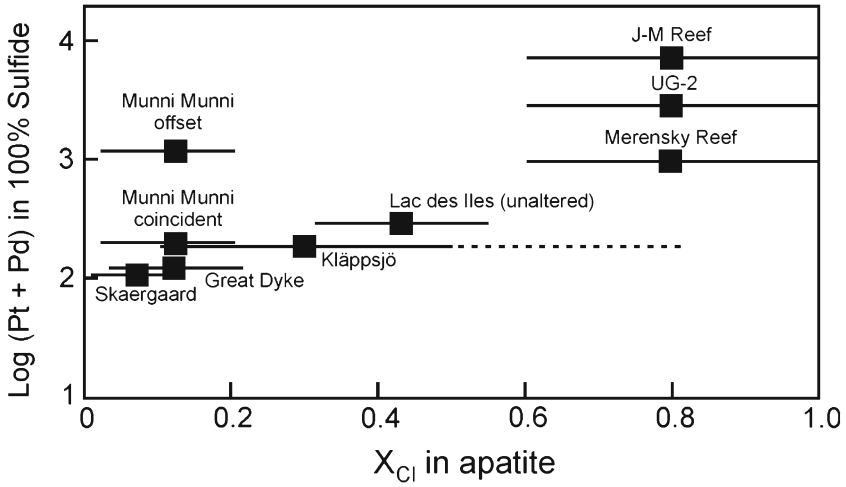

Fig. 6 Plot of the log (Pt + Pd) in 100 % sulfide fraction vs. chlorapatite component in and below the various reefs as shown. Kläppsjö PGE data from Meurer et al. (2004) and assumes 1 % average sulfide mode. Munni Munni PGE data from Barnes (1993). Skaergaard data from Andersen et al. (1998) and assumes 2 % average sulfide mode. Lac des Iles average PGE data from Barnes and Gomwe (2011). All other PGE data from Naldrett (2004). Apatite data from Boudreau (1995 and references therein), Meurer et al. (2004), and this study

Given the F-poor nature of the MBI apatite in mineralized rocks, the fluid-apatite composition is largely defined by the exchange reaction between apatite and an aqueous fluid in which HCl is present as neutral species:

$$\underset{\text{Apatite}}{OH-\text{apatite}} + \underset{\text{vapor}}{HCl^{\circ}} = \underset{\text{apatite}}{Cl-\text{apatite}} + \underset{\text{vapor}}{H_2O} \quad (1)$$

For a fixed activity of Cl and F in the vapor, the equilibrium exchange constant as a function of temperature, T, is given by the following equation (relevant thermodynamic data from 500 to 1,000 °C at 2.0 kbar (Zhu and Sverjensky 1992) and fitted to a linear equation in $1/T$):

$$\log K = \log\left(\frac{X^{Cl}_{apatite}\cdot a^{H_2O}_{fluid}}{X^{OH}_{apatite}\cdot a^{HCl^{\circ}}_{fluid}}\right) = 4,874/T(\text{Kelvin}) - 3.654 \quad (2)$$

Shown in Fig. 7 is a histogram of the MBI apatite, with calculated HCl/H_2O activity ratios. It is seen that even the relatively low Cl samples still contain substantial Cl in the vapor, a point also made by Hanley and Gladney (2011). Assuming that the activity ratios are approximately equal to concentration ratios, the calculated values are broadly similar to the experimental values of Webster et al. (2009) noted above.

A hydrothermal model

Given the potential for Cl-bearing fluids to transport the PGE, presented below is a first-order model for the evolution of the MBI mineralization by hydrothermal transport. It is shown schematically in Figs. 8 and 9.

1. Early zoned fluid migration stage (Fig. 8a): As the MBI can be described as a pipe-like, steeply plunging intrusion, solidification would be from the margins inward. At some stage during the solidification, the intrusion consists, from the margins toward the center, of (1) a relatively cool, fully solidified marginal rocks (± vapor), (2) a zone of solid + liquid + vapor, and (3) a hot central portion composed of solid + liquid that is not yet vapor-saturated.

   The early vapor that separates from the interstitial liquid is relatively H_2O- and Cl-rich (CO_2-poor) and carries with it S and the ore metals. This vapor is largely confined to the zone between the solidified margins and the not yet vapor-saturated core of the intrusion. Owing to the preferential location of mineralization along the southwestern side of the intrusion, it is suggested that the MBI had a steep plunge toward the southwest, and the fluids

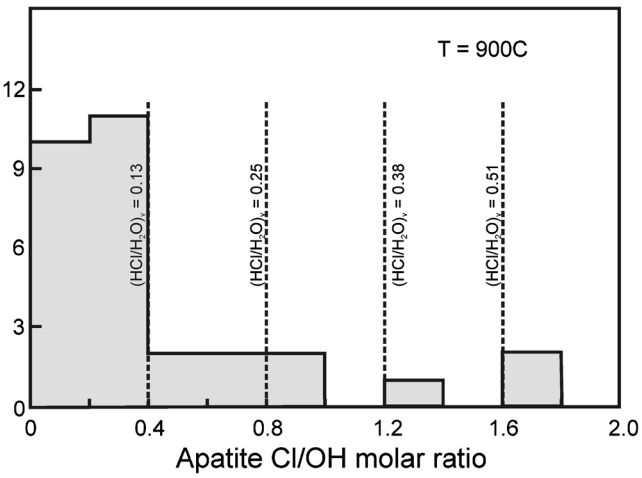

Fig. 7 Histogram of the Cl/OH molar ratio of apatite from the Mine Block Intrusion. *Dashed vertical lines* show the HCl/H_2O activity ratios calculated at 900 °C

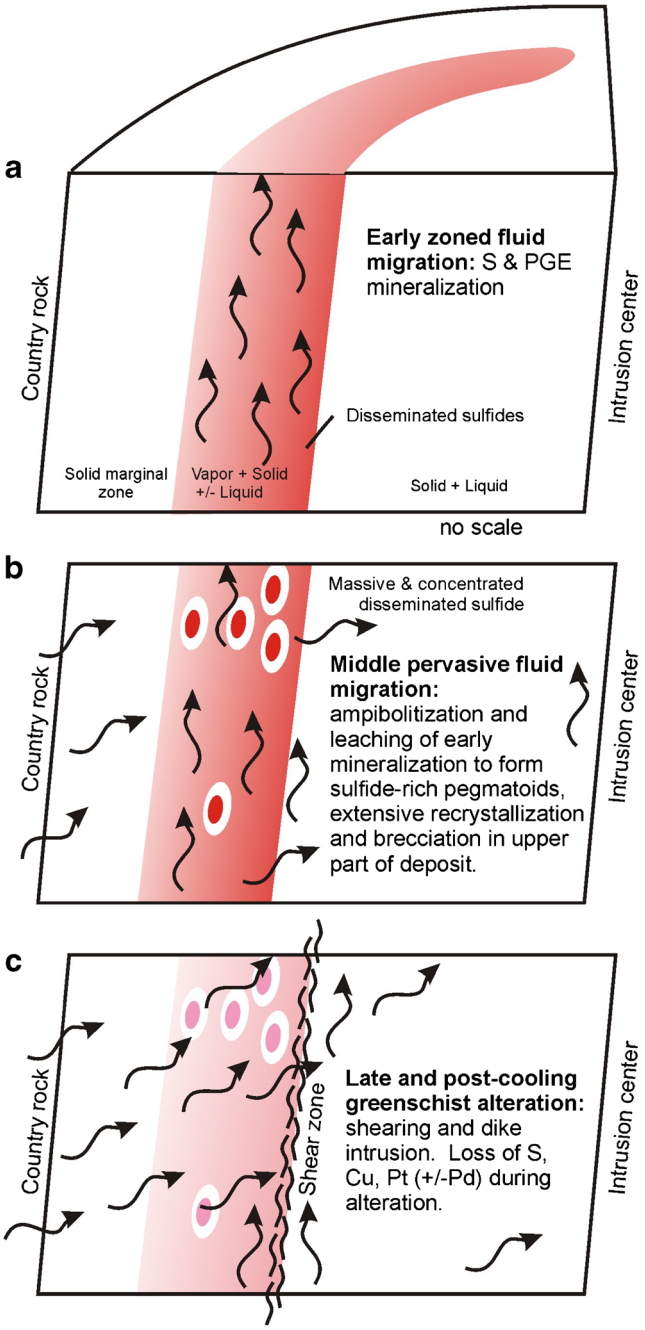

Fig. 8 Schematic hydrothermal model for the formation of the Mine Block Intrusion mineralization. See text for details

migrated upwards along the southwestern spine of the intrusion. Lateral heat loss leads to precipitation of disseminated PGE-sulfide to produce the mineralized norites.

Possible transport of mafic components by the Cl-bearing vapor may also lead to the enrichment of pyroxene to produce the higher grade melanorites just exterior to the East Gabbro. However, as discussed by Boudreau (1988) and Boudreau (1999), the addition of C-O-H-S vapor to vapor-undersaturated interstitial silicate liquids will have several effects: (1) The redissolution of vapor will add S to the liquid and drive it to sulfide saturation. (2) Hydrated silicate liquid tends to stabilize mafic relative to felsic minerals: the addition of H_2O to interstitial liquid leads to preferential dissolution of plagioclase relative to mafic minerals, resulting in the formation of the melanorites as the East Gabbro is approached. (3) Mixing of the hydrated interstitial liquids, which are now relatively enriched in the plagioclase component, with the more interior, hotter, and dryer liquids, leads to preferential saturation of plagioclase to produce the leuconorite of the East Gabbro.

The effects of H_2O on liquidus phase assemblages are illustrated in Fig. 9. Shown is the ternary system anorthite-B-H_2O, which is a section of the four-component system anorthite-forsterite-silica-H_2O (after Kushiro et al. 1968; Kushiro 1975). Point B is the intercept of the tieline connecting anorthite and the initial (dry cotectic) anorthite + enstatite-saturated liquid projected to the forsterite-SiO_2 sideline, as shown in the inset at the upper right of the figure. Projected onto this ternary are both the bulk solid and the bulk solid + liquid assemblages, as noted. Addition of an H_2O-rich vapor to the initially vapor-undersaturated bulk composition leads to migration of the bulk composition towards the H_2O apex as illustrated in Fig. 9a. As long as liquid anorthite and enstatite are all present, a tieline from the bulk solid and the evolving liquid is constrained to pass through bulk solid, as is shown. The result is the preferential melting of anorthite and the production of an enstatite-rich restite (residual solid assemblage). As similarly described by Boudreau (1999) at higher degrees of partial melting, olivine can also occur, and this can explain the possible presence of this mineral suggested by bulk rock compositions reported by Barnes and Gomwe (2011). The more vapor added, the more enriched is the restite in enstatite (±olivine and clinopyroxene) and, as noted above, the more PGE-sulfide precipitated. Thus, the High-Grade Zone and the excess pyroxene at the contact with the East Gabbro are interpreted to both having resulted from the same vapor mixing event: the higher grades and more melanocratic rocks formed where more fluid mixed in with fluid-undersaturated interstitial liquids to produce the high-grade "pyroxenite" unit by hydration melting and preferential loss of plagioclase.

As the hydrated silicate liquid produced by hydration melting moves away from the region of

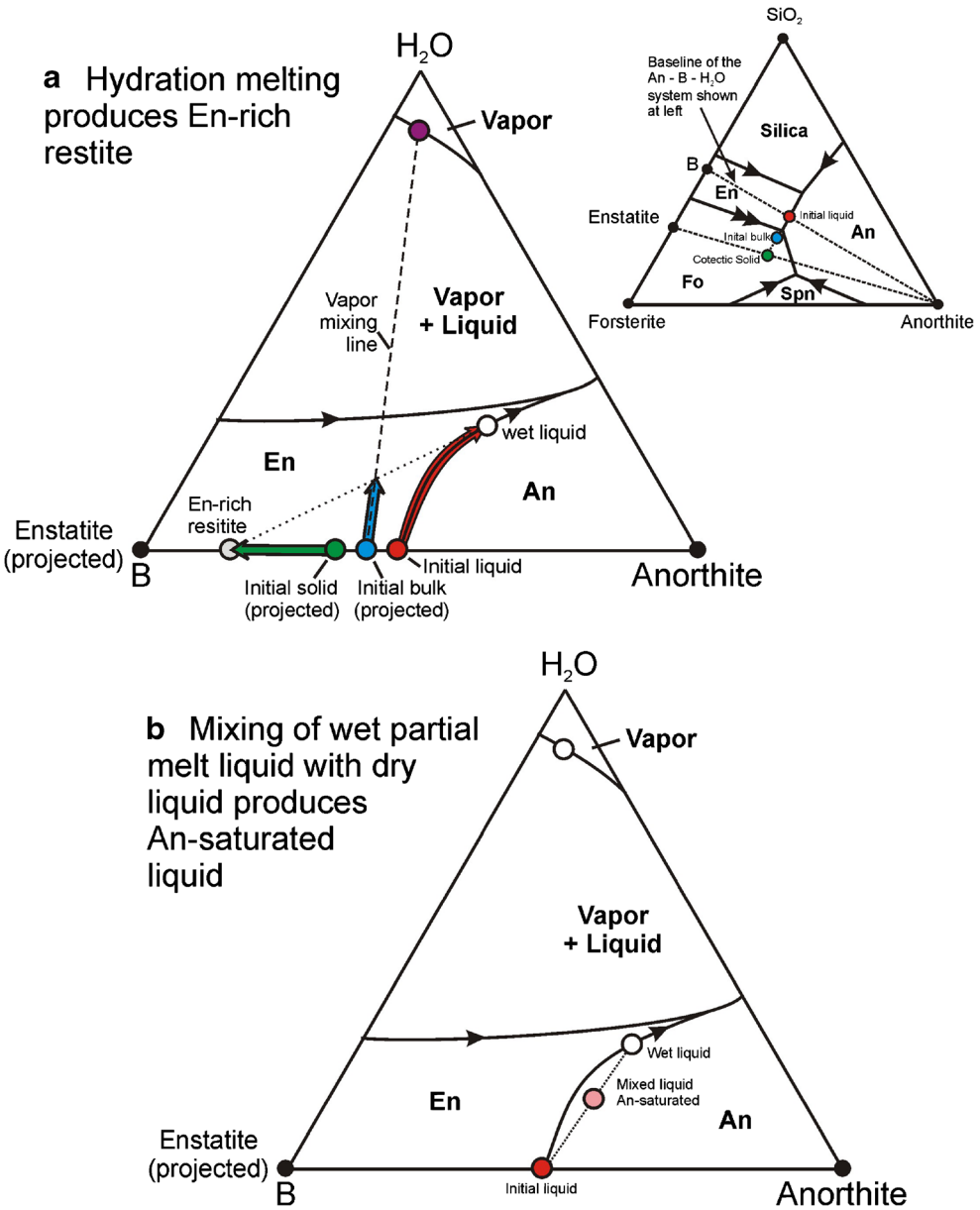

Fig. 9 Schematic model for the modal variations in plagioclase and pyroxene in the transition from melanorite/pyroxenite to the leucocratic East "Gabbro". **a** The system anorthite-B-H_2O, where B is the intercept of the anorthite–initial (dry cotectitc) anorthite + enstatite-saturated liquid tieline projected to the forsterite-SiO_2 sideline as shown in the *inset at the upper right*. Addition of H_2O to the initially dry bulk composition leads to hydration melting and the production of an enstatie-rich resitite (residual solid assemblage). **b** Same system as for **a** but illustrating the mixing of the wet partial melt with the original dry cotectic liquid to produce an anorthite-saturated hybrid liquid. See text for detailed discussion

hydration (by interstitial liquid convection), the hydrated partial melt can mix in with dryer interstitial liquid that has not been affected by the hydration event. The mixing of these two liquids produces a hydrated liquid that is saturated in plagioclase alone, as is illustrated in Fig. 9b. (More formerly, as the interstitial liquid is buffered by the presence of plagioclase and pyroxene, the result is that the liquid will be constrained to the cotectic by dissolution of pyroxene and precipitation of plagioclase, but the result will still be the preferential enrichment in plagioclase). The result is the production of the leucocratic East "Gabbro" that is enriched in the plagioclase component lost from the mineralized melanorite unit.

2. Middle fluid migration stage—amphibolitization (Fig. 8b): Continued degassing of the interstitial liquid from deeper levels (and possibly some infiltrating country fluids) results in these later fluids being markedly poorer in Cl. With continued cooling, amphibole becomes stable, and reaction of this late fluid with original norites results in locally extensive amphibolitization and leaching of Cl from earlier precipitated apatite. Dehydration of the vapor during amphibolitization causes an increase in the CO_2/H_2O ratio of the fluid (Boudreau et al. 2014), producing the CO_2-rich fluid inclusions associated with the amphibolite pegmatoids described by Hanley and Gladney (2011). The combined effect is a partial remobilization of the original disseminated sulfide and concentration into locally developed sulfide amphibolite pegmatoids.

At this stage, vapor infiltration is locally variable. Because of the reactive nature of these fluids, other effects include the extensive development of heterolithic and varitextured rocks, particularly towards the surface (the upper part of the Roby and nearby Twilight Zones). These heterolithic units, which are defined mainly by variations in the proportions of plagioclase and pyroxene (Barnes and Gomwe 2011), are assumed to be formed by the same process that formed the mafic/felsic replacement bodies of the Skaergaard Intrusion (McBirney and Sonnenthal 1990).

3. Late and post-cooling greenschist alteration (Fig. 8c): Fluid inclusion and stable isotopic data of Somarin et al. (2009) suggest that cooling of the MBI onto greenschist conditions involved the mixing of county fluids with residual magmatic fluids. During the final cooling of the intrusion (and during any post-cooling events), fluid alteration resulted in locally extensive greenschist alteration to chlorite + tremolite/actinolite ± talc ± epidote assemblages, particularly along shears concentrated between melanorite of the varitextured zone and pyroxenite outbound of the more leucocratic rocks of the East Gabbro. The net effect, as discussed by Boudreau et al. (2014) is the progressive loss of S, the base metals, and the PGE with increasing alteration.

Conclusions

Apatites from the fresher rocks of the Mine Block Intrusion are enriched in Cl as compared with those affected by amphibolite and lower grade alteration. The presence of elevated Cl in this and other PGE zones in mafic intrusions suggests an important role for Cl-bearing fluids in the transport of sulfur and the PGE. In regards to the high Pd/Ir ratio of the MBI mineralization, it is suggested that the relatively hydroxyapatite-rich nature of the MBI apatite is consistent with the existence of a Cl-bearing but relatively H_2O-rich (CO_2-poor) fluid. Given the experimental evidence that high concentrations of both Cl and CO_2 are required to move the IPGE, the intermediate concentrations of these two components in the MBI fluid instead strongly limited the transport of the less soluble IPGE.

Acknowledgments The two Duke University authors would like to thank North American Palladium for their support of this project. This work was completed as part of a Duke University Senior Thesis by the senior author. It has been substantially improved by the efforts of two anonymous reviewers, whose efforts are very much appreciated.

References

Andersen JCØ, Rasmussen H, Nielsen TFD, Ronsbo JG (1998) The triple group and the Platinova gold and palladium reefs in the Skaergaard intrusion: stratigraphic and petrographic relations. Econ Geol 93: 488–509

Barnes SJ (1993) Partitioning of the platinum group elements and gold between silicate and sulphide magmas in the Munni Munni Complex, Western Australia. Geochim Cosmochim Acta 57:1277–1290

Barnes S-J, Gomwe TS (2011) The Pd deposit of the Lac des Iles Complex, Northwestern Ontario. Rev Econ Geol 17:351–370

Blaine FA (2010) The effect of volatiles (H2O, Cl and CO2) on the solubility and partitioning of platinum and iridium in fluid–melt systems. PhD Dissertation, University of Waterloo, 170 pp

Blaine FA, Linnen RL, Holtz F, Bruegmann GE (2005) Platinum solubility in a haplobasaltic melt at 1250°C and 0.2 GPa: the effect of water content and oxygen fugacity. Geochim Cosmochim Acta 69: 1265–1273

Boudreau AE (1988) Investigations of the Stillwater Complex, IV. The role of volatiles in the petrogenesis of the J-M reef, Minneapolis adit section. Can Mineral 26:193–208

Boudreau AE (1995) Fluid evolution in layered intrusions: evidence from the chemistry of the halogen-bearing minerals. In: Magmas, fluids, and ore deposits (J.F.H. Thompson, ed.). Mineral Ass Can Short Course 26:25–45

Boudreau AE (1999) Fluid fluxing of cumulates: the J-M reef and associated rocks of the Stillwater Complex, Montana. J Petrol 40: 755–772

Boudreau AE, McCallum IS (1989) Investigations of the Stillwater Complex: part V. Apatite as indicators of evolving fluid composition. Contrib Mineral Petrol 102:138–153

Boudreau AE, McCallum IS (1990) Low temperature alteration of REE-rich chlorapatite from the Stillwater Complex, Montana. Am Mineral 75:687–693

Boudreau AE, McCallum IS (1992) Concentration of Platinum-group elements by magmatic fluids in layered intrusions. Econ Geol 87: 1830–1848

Boudreau AE, Mathez EA, McCallum IS (1986) Halogen geochemistry of the Stillwater and Bushveld Complexes: evidence for transport of the platinum-group elements by Cl-rich fluids. J Petrol 27:967–986

Boudreau AE, Djon L, Ychalikian A, Corkery J (2014) The Lac Des Iles Palladium Deposit, Ontario, Canada. Part I. The effect of variable alteration on the Offset Zone. Mineral Deposita 49:625–654

Brügmann GE, Naldrett AJ, Macdonald AJ (1989) Magma mixing and constitutional zone-refining in the Lac-Des-Iles Complex, Ontario —genesis of platinum-group element mineralization. Econ Geol 84: 1557–1573

Brügmann GE, Reischrnann T, Naldrett AJ, Sutcliffe RH (1997) Roots of an Archean volcanic arc complex; the Lac des îles area in Ontario, Canada. Precambrian Res 81:223–239

Djon MLN, Barnes S-J (2012) Changes in sulfides and platinum-group minerals with the degree of alteration in the Roby, Twilight, and High Grade Zones of the Lac des Iles Complex, Ontario, Canada. Miner Deposita 47:875–896

Dunning GR (1979) The geology and platinum-group mineralization of the Roby Zone, Lac des îles Complex, Northwestern Ontario. MSc thesis, University of Toronto

Duran CJ, Barnes S-J, Corkery JT (2012) Petrogenesis of massive sulphides from the Lac-des-Iles Palladium ore deposits, Western Ontario, Canada. 2th IntNi-Cu-(PGE) Symp, Guiyang, China, 18–19 June 2012. Abstract

Frondel JW (1964) Variations of some rare earth elements in allanite. Am Mineral 49:1159–1177

Gomwe ST (2008) The formation of the palladium-rich Roby, Twilight and High Grade Zones of the Lac des Iles Complex. PhD Thesis, Université du Québec à Chicoutimi

Hanley JJ, Gladney ER (2011) the presence of carbonic-dominant volatiles during the crystallization of sulfide-bearing mafic pegmatites in the North Roby Zone, Lac des Iles Complex, Ontario. Econ Geol 106:33–54

Hanley JJ, Pettke T, Mungall JE, Spooner ETC (2005) The solubility of platinum and gold in NaCl brines at 1.5 kbar, 600 to 800°C: a laser ablation ICP-MS pilot study of synthetic fluid inclusions. Geochim Cosmochim Acta 69:2593–2611

Hinchey JG, Hattori KH (2005) Magmatic mineralization and hydrothermal enrichment of the High Grade Zone at the Lac des Iles palladium mine, northern Ontario, Canada. Miner Deposita 40:13–23

Hinchey JG, Hattori KH, Langne MJ (2005) Geology, petrology, and controls on PGE mineralization of the southern Roby and Twilight zones, Lac des Iles mine, Canada. Econ Geol 100:43–61

Hoover JD (1989) Petrology of the Marginal Border Series of the Skaergaard intrusion. J Petrol 30:399–439

Hovis GL, Harlov DE (2010) Solution calorimetric investigation of fluorchlorapatite crystalline solutions. Am Min 95:946–952

Hsu LC, Lechler PJ, Nelson JH (1991) Hydrothermal solubility of palladium in chloride solutions from 300° to 700° C: Preliminary experimental results. Econ Geol 86:422–427

Kushiro I (1975) On the nature of silicate melt and its significance in magma genesis: regularities in the shift of the liquidus boundaries involving olivine, pyroxene, and silica minerals. Am J Sci 275:411–431

Kushiro I, Yoder HS, Nishikawa M (1968) Effect of water on the melting of enstatite. Geol Soc Am Bull 79:1685–1692

Lavigne MJ, Michaud MJ (2001) Geology of North American Palladium Ltd's Roby Zone Deposit, Lac des Iles. Explor Min Geol 10:1–17

Mathez EA, Webster JD (2005) Partitioning behavior of chlorine and fluorine in the system apatite–silicate melt–fluid. Geochim Cosmochim Acta 69:1275–1286

McBirney AR, Sonnenthal EL (1990) Metasomatic replacement in the Skaergaard Intrusion, East Greenland: preliminary observations. Chem Geol 88:245–260

Meurer WP, Boudreau AE (1996) Evaluation of models for halogen variations in apatite from layered intrusions using a detailed study of apatite from OB-III and OB-IV of the Middle Banded series, Stillwater Complex, Montana. Contrib Mineral Petrol 123:225–236

Meurer WP, Meurer MES (2006) Using apatite to dispel the "trapped liquid" concept and to understand the loss of interstitial liquid by compaction in mafic cumulates: an example from the Stillwater Complex, Montana. Contrib Mineral Petrol 151:187–201

Meurer WP, Helström FA, Claeson DT (2004) The relationship between chlorapatite and PGE-rich cumulates in layered intrusions: the Kläppsjö Gabbro, North-Central Sweden, as a case study. Can Mineral 42:279–289

Morton RD, Cantanzaro EJ (1974) Stable chlorine isotope abundances in apatite from Odegårdens Verk, Norway. Norsk Geologisk Tidsskrift 44:307–313

Naldrett AJ (2004) Magmatic sulfide deposits: geology, geochemistry and exploration. Springer, New York, 727 pp

Pye EG (1968) Geology of the Lac des îles area, District of Thunderbay. Ontario Dept Mines Geol Report 64, 47 pp

Roeder PL (1985) Electron-microprobe analysis of minerals for rare-earth elements: Use of calculated peak-overlap corrections. Can Mineral 23:263–271

Simon AC, Pettke T (2009) Platinum solubility and partitioning in a felsic melt – vapor – brine assemblage. Geochim Cosmochim Acta 73: 438–454

Somarin AK, Kissin SA, Heerema DD, Bihari DJ (2009) Hydrothermal alteration, fluid inclusion and stable isotope studies of the North Roby zone, Lac des Iles PGE mine, Ontario, Canada. Resour Geol 59:107–120

Stone D (2010) Precambrian geology of the central Wabigoon Subprovince area, northwestern Ontario. Ont Geol Sur Open File Report 5422:130

Stone D, Lavigne MJ, Schnieders B, Scott J, Wagner D (2003) Regional geology of the Lac des Iles area. Summary of field work and other activities open file report 6120, Ontario Geological Survey

Stormer JC, Pierson ML, Tacker RC (1993) Variation of F and Cl X-ray intensity due to anisotropic diffusion in apatite during electron microprobe analysis. Am Mineral 78:641–648

Sutcliffe RH, Sweeny JM, Edgar AD (1989) The Lac des Iles Complex, Ontario: petrology and platinum-group-elements mineralization in an Archean mafic intrusion. Can J Earth Sci 26:1408–1427

Tacker RC, Stormer JC (1989) A thermodynamic model for apatite solid solutions, applicable to high-temperature geologic problems. Am Mineral 74:877–888

Talkington RW, Watkinson DH (1984) Trends in the distribution of the precious metals in the Lac-Des-Iles Complex, Northwestern Ontario. Can Mineral 22:125–136

Watkinson D H, Lavigne MJ, Fox PE (2002) Magmatic-hydrothermal Cu- and Pd-rich deposits in Gabbroic Rocks from North America. In: Cabri LJ (ed) The geology, geochemistry, mineralogy and mineral beneficiation of platinum-group elements. Can Inst Min Metall 54:299–320

Webster JD, Tappen CM, Mandeville CW (2009) Partitioning behavior of chlorine and fluorine in the system apatite–melt–fluid. II: Felsic silicate systems at 200 MPa. Geochim et Cosmochim Acta 73:559–581

Willmore CC, Boudreau AE, Kruger FJ (2000) The halogen geochemistry of the Bushveld Complex, Republic of South Africa: implications for chalcophile element distribution in the lower and critical zones. J Petrol 41:1517–1539

Zhu C, Sverjensky DA (1992) F-Cl-OH partitioning between biotite and apatite. Geochim Cosmochim Acta 56:3435–3468